



Cite this: *J. Mater. Chem. A*, 2017, 5, 23987

## Mapping a stable solvent structure landscape for aprotic Li–air battery organic electrolytes†

Shuting Feng, <sup>a</sup> Mao Chen, <sup>b</sup> Livia Giordano, <sup>c</sup> Mingjun Huang, <sup>b</sup> Wenvu Zhang, <sup>b</sup> Chibueze V. Amanchukwu, <sup>a</sup> Robinson Anandakathir, <sup>d</sup> Yang Shao-Horn <sup>\*c</sup> and Jeremiah A. Johnson <sup>\*b</sup>

Electrolyte instability is one of the greatest impediments that must be overcome for the practical development of rechargeable aprotic Li–air batteries. In this work, we establish a comprehensive framework for evaluation of the stability of potential organic electrolytes for aprotic Li–air batteries that is based on four key descriptors: Bond dissociation energy, deprotonation free energy (*i.e.*, Acidity), Nucleophilic substitution free energy, and Electrochemical oxidation/reduction. These parameters were calculated for several classes of organic compounds. The chemical stability of the molecules was studied experimentally under conditions designed to mimic the aprotic Li–air battery environment (heating in the presence of excess  $\text{KO}_2$  and  $\text{Li}_2\text{O}_2$ ). In general, the calculated and experimental data agreed well for alkanes, alkenes, ethers, aromatics, carbonates, and S-containing and N-containing compounds. Using this dataset, we identified functional groups and other structural features of organic molecules that may be suitable for aprotic Li–air battery electrolyte design.

Received 20th September 2017  
 Accepted 1st November 2017

DOI: 10.1039/c7ta08321a  
[rsc.li/materials-a](http://rsc.li/materials-a)

## Introduction

Li–air batteries have attracted vast research attention due to their high theoretical specific energy and potential in transportation applications. Currently, the development of aprotic Li–air batteries is hindered by a number of challenges amongst which electrolyte instability is one of the most important to overcome before a practical battery can be realized.<sup>1–3</sup> Numerous families of organic molecules,<sup>4–18</sup> polymers,<sup>19–22</sup> and ionic liquids<sup>23,24</sup> have been examined in this context; none are stable against the oxygen electrode in  $\text{Li}^+$ – $\text{O}_2$  batteries. Therefore, increasing the chemical stability of electrolytes in the  $\text{Li}^+$ – $\text{O}_2$  electrode is critical to develop stable electrolytes for aprotic Li–air batteries.

Carbonate solvents (*e.g.*, propylene carbonate) that are used in Li-ion batteries are unstable against nucleophilic substitution<sup>4,6,11</sup> during discharge of aprotic Li– $\text{O}_2$  batteries, where superoxide ( $(\text{O}_2^-)^{25}$  and  $(\text{Li}^+ - \text{O}_2^-)^{25,26}$ ) and peroxide ( $\text{Li}_2\text{O}_2$ )<sup>25,26</sup>

are formed upon the reduction of molecular oxygen. In addition, polymers commonly used in Li-ion batteries have been shown to be unstable against superoxide and peroxide.<sup>19–21</sup> For instance, superoxide reacts with poly(vinylidene difluoride) (PVdF), which causes dehydrofluorination and the formation of  $\text{H}_2\text{O}_2$ .<sup>19</sup> Vinyl polymers such as poly(acrylonitrile) (PAN) and poly(vinyl chloride) (PVC) are subject to nucleophilic attack by superoxide.<sup>20</sup> Amanchukwu *et al.*<sup>21</sup> have evaluated the reactivity between  $\text{Li}_2\text{O}_2$  and numerous polymers such as PVDF, PAN, PVC, poly(methyl methacrylate) (PMMA), poly(tetrafluoroethylene) (PTFE), Nafion, and poly(ethylene oxide) (PEO), and have proposed that polymers with highly electron-withdrawing functional groups on the side chain are susceptible to decomposition in the presence of  $\text{Li}_2\text{O}_2$ . While ether-based small molecule and polymer electrolytes<sup>10,22</sup> and certain room-temperature ionic liquids (RTILs)<sup>23,24</sup> exhibit higher stability than carbonates during discharge, ether-based electrolytes might be susceptible to hydrogen abstraction by superoxide<sup>10</sup> and RTIL cations with hydrogens  $\beta$  to a nitrogen atom can undergo elimination upon deprotonation by superoxide.<sup>23</sup> Recent density functional theory (DFT) studies have elucidated reaction mechanisms of electrolyte decomposition.<sup>6,7,14,17,27–33</sup> For example, Bryantsev and coworkers<sup>7,14,17</sup> have screened the solvent susceptibility against nucleophilic substitution by superoxide using the activation free energies ( $\Delta G_{\text{act}}^\ddagger$ ) and reaction free energies ( $\Delta G_{\text{nuc}}$ ), and against deprotonation using  $pK_a$  values of different organic solvents. These researchers have reported that the *O*-alkyl and *S*-alkyl carbons are favourable sites of nucleophilic substitution by superoxide in a wide range of

<sup>a</sup>Department of Chemical Engineering, Massachusetts Institute of Technology, 77 Massachusetts Avenue, Cambridge, MA 02139, USA

<sup>b</sup>Department of Chemistry, Massachusetts Institute of Technology, 77 Massachusetts Avenue, Cambridge, MA 02139, USA. E-mail: [jaj2109@mit.edu](mailto:jaj2109@mit.edu)

<sup>c</sup>Department of Mechanical Engineering, Massachusetts Institute of Technology, Cambridge, MA 02139, USA. E-mail: [shaohorn@mit.edu](mailto:shaohorn@mit.edu)

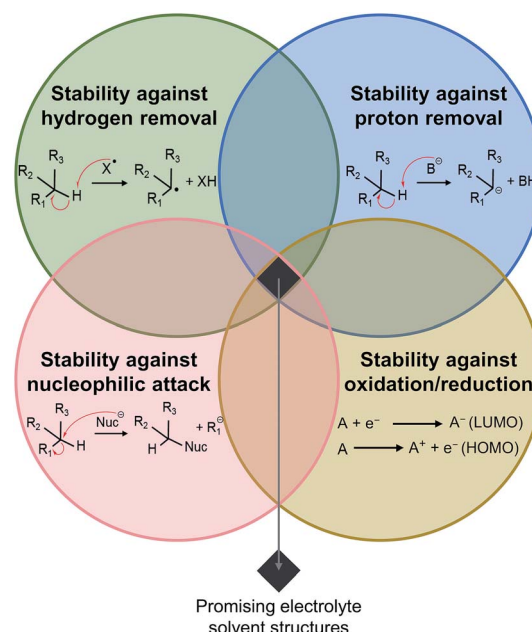
<sup>d</sup>Samsung Advanced Institute of Technology (SAIT), 3 Van de Graaff Drive, Burlington, MA 01803, USA

† Electronic supplementary information (ESI) available. See DOI: [10.1039/c7ta08321a](https://doi.org/10.1039/c7ta08321a)

‡ These authors contributed equally.

organic solvents including organic carbonates, sulfonate esters, carboxylic esters, lactones, and sulfones.<sup>7,14</sup> Additionally, the  $\alpha$ -hydrogens in esters, short-chain dinitriles, and *N*-alkyl imides are relatively acidic and susceptible to deprotonation by superoxide.<sup>14,17</sup> Among the solvents screened, superior stability against nucleophilic substitution and deprotonation are found in *N,N*-dialkyl amides and glymes.<sup>7,14,17</sup> However, these molecules are known to be susceptible to C–H bond homolytic cleavage by molecular oxygen,<sup>27</sup> highlighting the need to simultaneously consider and screen bond dissociation energies for hydrogen abstraction. Unfortunately, these computational studies have only considered one or two possible decomposition mechanisms and selected different sets of solvents for their investigations; they do not provide a comprehensive evaluation of solvent chemical stability. Moreover, having greater positive carbon atomic charge has been used as an indicator for increasing susceptibility to nucleophilic attack by superoxide.<sup>28–30</sup> For instance, Katayama *et al.*, reported that the carbon atom in an imidazolium cation most vulnerable to nucleophilic substitution (the 2 position) exhibits the highest positive charge, suggesting a correlation between positive carbon atomic charge and susceptibility to nucleophilic attack by superoxide in this class of cationic compounds.<sup>30</sup> Nevertheless, Bryantsev *et al.*<sup>7</sup> claim no significant correlation between the computed atomic charges and activation free energies of nucleophilic attack on organic solvents such as ethers, nitriles, and amides. Besides chemical stability against oxygen and its reduction products, suitable electrolytes must also be electrochemically stable at  $\sim 4.0$  V<sub>Li</sub>. Numerous experimental and computational studies show that well-known organic electrolytes such as carbonates<sup>31–37</sup> and ethers<sup>31–35,37</sup> are stable against electrochemical oxidation at 4.0 V<sub>Li</sub> or higher, rendering chemical stability the most limiting factor for their application in Li–O<sub>2</sub> batteries. Nonetheless, new electrolyte design may enter the electrochemical stability limiting regime. In light of the tremendous degrees of freedom in electrolyte selection and discovery, high-throughput ( $>1000$  organic molecules) computations based on redox potentials, solvation energies, and structural changes have been employed to accelerate the search of optimal electrolyte materials.<sup>38</sup> However, as pointed out by Cheng *et al.*, more detailed studies of specific reaction mechanisms utilizing a smaller set of structural candidates are needed for Li–O<sub>2</sub> batteries, as electrolytes can react with the discharge products or intermediate radical species in the Li–O<sub>2</sub> environment.<sup>38</sup> In this study, we seek a global assessment of chemical and electrochemical stability in a wide range of solvent families in the Li<sup>+</sup>, O<sub>2</sub> electrode of aprotic Li–O<sub>2</sub> batteries. We note that electrolyte instability against metallic lithium is a critical and challenging issue that merits its own forum and lies outside the scope of this manuscript.

Herein, we introduce a framework for comprehensive assessment of the stability of organic molecules in the aprotic Li<sup>+</sup>, O<sub>2</sub> electrode. This framework, referred to as “BANE”, makes use of four stability descriptors (Scheme 1): (1) Bond dissociation energy (BDE), which predicts the likelihood of hydrogen abstraction by radicals in the aprotic Li<sup>+</sup>, O<sub>2</sub> electrode environment; (2) deprotonation free energy (a.k.a. Acidity), which



Scheme 1 The “BANE” paradigm for assessing the stability of organic molecules in the Li–O<sub>2</sub> battery environment. BANE uses calculated Bond dissociation energies, Acidity (deprotonation free energies), Nucleophilic substitution free energy, and Electrochemical stability to predict the susceptibility of molecules to hydrogen abstraction, deprotonation, nucleophilic substitution, and reduction/oxidation.

predicts the likelihood of deprotonation and base-induced elimination reactions in the aprotic Li<sup>+</sup>, O<sub>2</sub> electrode; (3) Nucleophilic substitution reaction free energy, which predicts the driving force for nucleophilic attack by species such as superoxide; and (4) Electrochemical stability as predicted by oxidation and reduction energies in solution. Stable electrolytes for the aprotic Li<sup>+</sup>, O<sub>2</sub> electrode should ideally have high BDEs and deprotonation free energies for every hydrogen/proton, high stability against nucleophilic substitution, and high stability ( $>4.0$  V<sub>Li</sub>) against electrochemical oxidation. We employ DFT to compute the BDEs, deprotonation free energies, Natural Population Analysis (NPA) atomic charges, and redox potentials associated with 32 neutral small molecules selected from several different families of organic molecules including carbonates, ethers, S-containing molecules (sulfoxides, sulfones, and thioethers), N-containing molecules (amides and amines), alkanes, alkenes, and aromatics (Fig. 1). These small molecules bear varied functional groups, which allow us to assess the effects of chemical structure and composition on bond strength, acidity, atomic partial charge, and redox stability as well as the potential interplay among these factors. The free energies of nucleophilic substitution of selected molecules by superoxide have also been calculated, from which the predicting power of NPA partial atomic charge on the susceptibility against nucleophilic substitution has been examined. Furthermore, the correlation between the computed oxidation energies and the NPA partial atomic charges has been explored. Collectively, the BANE paradigm allows us to identify structural motifs that are likely to be stable in the aprotic Li<sup>+</sup>, O<sub>2</sub> electrode, and in

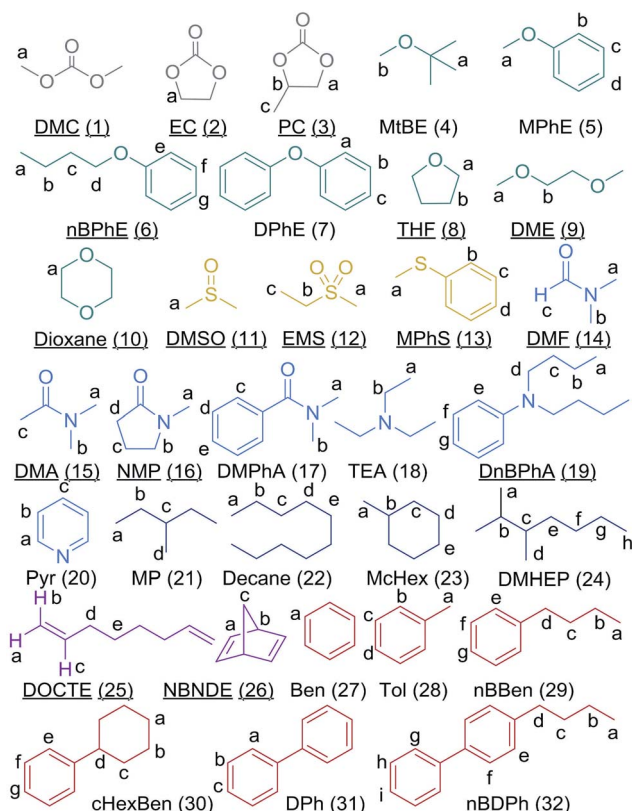


**Fig. 1** Structures considered in this work were selected from several different families of organic compounds: carbonates, ethers, S-containing molecules, N-containing molecules, alkanes, alkenes, and aromatics. Non-equivalent protons/hydrogens are labelled. Compounds with lines under their name were found to be unstable in our experimental chemical stability tests.

cases where instability has been predicted it is possible to propose a likely decomposition reaction mechanism. Experimental chemical stability tests were conducted to validate the computed predictions; excellent agreement between experimental observations and our computations was observed. Altogether, the BANE approach illuminates molecular-level structure–property relationships that should guide the design of stable organic electrolytes for aprotic Li–O<sub>2</sub> batteries.

## Computational and experimental methods

### Theoretical calculations

All calculations were performed using the Gaussian 09 computational package.<sup>39</sup> All geometries were optimized using B3LYP/6-31G(d,p),<sup>40,41</sup> and the ground states were verified by the absence of imaginary frequencies. In addition, single point energies were obtained at the B3LYP/6-311++G(d,p) level of theory for NPA, nucleophilic substitution reaction free energy, ionization potential (IP), and electron affinity (EA) calculations. The solvation effects were captured implicitly using the conductor-like polarizable continuum model (CPCM)<sup>42,43</sup> with dimethyl sulfoxide (DMSO) as the universal solvent. DMSO was

selected because it is commonly used in Li–O<sub>2</sub> batteries and experimental acidity data of organic molecules is available in DMSO (Bordwell pK<sub>a</sub> Table<sup>44</sup>).

BDE was calculated as the Gibbs free energy associated with the solution-phase homolytic cleavage of a C–H bond, which is expressed as

$$\text{BDE} = G(\text{RC}'_{(s)}) + G(\text{H}'_{(s)}) - G(\text{RC}-\text{H}_{(s)})$$

where  $G(\text{RC}'_{(s)})$ ,  $G(\text{H}'_{(s)})$ , and  $G(\text{RC}-\text{H}_{(s)})$  are the Gibbs free energies of  $\text{RC}'$ ,  $\text{H}'$ , and  $\text{RC}-\text{H}$  in implicit DMSO solvent, respectively. The solution phase deprotonation energies were estimated using the thermodynamic cycles shown in Fig. S1,<sup>†</sup> where

$$\Delta G_{\text{deprot}} = \Delta G_{g,\text{deprot}} + \Delta G_s(\text{RC}^-) + \Delta G_s(\text{H}^+) - \Delta G_s(\text{RC}-\text{H})$$

where  $\Delta G_{\text{deprot}}$  and  $\Delta G_{g,\text{deprot}}$  are the solution- and gas-phase deprotonation energies, respectively.  $\Delta G_s(\text{RC}^-)$ ,  $\Delta G_s(\text{H}^+)$ , and  $\Delta G_s(\text{RC}-\text{H})$  are the solvation free energies of  $\text{RC}^-$ ,  $\text{H}^+$ , and  $\text{RC}-\text{H}$ , respectively. Because the liquid-phase solvation free energy calculations employ an ideal solution at 1 M as the reference, while gas-phase free energy calculations use a reference state of an ideal gas at 1 atm, the following unit conversion between the gas-phase and liquid-phase was used

$$\Delta G_g(1 \text{ M}) = \Delta G_g(1 \text{ atm}) + RT \ln(24.46)$$

Employing this conversion, the final expression for solution-phase  $\Delta G_{\text{deprot}}$  is

$$\begin{aligned} \Delta G_{\text{deprot}} &= G(\text{RC}'_{(g)}) + G(\text{H}'_{(g)}) - G(\text{RC}-\text{H}_{(g)}) + RT \ln(24.46) \\ &\quad + \Delta G_s(\text{RC}^-) + \Delta G_s(\text{H}^+) - \Delta G_s(\text{RC}-\text{H}) = G(\text{RC}'_{(s)}) \\ &\quad + G(\text{H}'_{(g)}) - G(\text{RC}-\text{H}_{(s)}) + RT \ln(24.46) + \Delta G_s(\text{H}^+) \end{aligned}$$

A value of  $-1143.45 \text{ kJ mol}^{-1}$  for  $\Delta G_s(\text{H}^+)$  in DMSO was used.<sup>45</sup>

We computed the reaction free energies of nucleophilic substitution ( $\Delta G_{\text{nuc}}$ ) of selected organic molecules by superoxide, and investigated whether carbon partial atomic charges obtained by NPA can reliably predict the  $\Delta G_{\text{nuc}}$ .

The likelihood of oxidation was estimated by oxidation energy calculation, which is the Gibbs free energy for the reaction  $\text{M} \rightarrow \text{M}^+ + \text{e}^-$  in the solution. The reduction energy, which corresponds to the reaction  $\text{M} + \text{e}^- \rightarrow \text{M}^-$ , was also calculated. The oxidation and reduction energies,  $G_{\text{Ox}}$  and  $G_{\text{Re}}$ , are defined as

$$G_{\text{Ox}} = G(\text{M}^+) - G(\text{M})$$

$$G_{\text{Re}} = G(\text{M}^-) - G(\text{M})$$

The calculations of adiabatic redox energies allowed for geometry optimization of the charged states. A graphical comparison between adiabatic and vertical oxidation energy is shown in Scheme S1.<sup>†</sup>

## Experimental details

### Material and instrument information

$\text{KO}_2$ ,  $\text{Li}_2\text{O}_2$ , solvents, and all organic compounds tested in this work were purchased from Sigma-Aldrich or Alfa Aesar (99% purity or greater), and were used directly without further purification. Nuclear magnetic resonance (NMR) spectra were recorded on a Bruker AMX 400 MHz NMR spectrometer.  $^1\text{H}$  NMR signals were measured relative to the signal for residual DMSO (2.5 ppm) in  $d_6$ -DMSO, *N,N*-dimethylformamide (DMF; 2.92 and 2.75 ppm) in  $d_7$ -DMF, or chloroform (7.26 ppm) in  $\text{CDCl}_3$ , and are reported in  $\delta$  units, parts per million (ppm).

### General procedure for chemical stability screening

A 10 mL microwave vial containing a stir bar was charged with the compound of interest (5 mmol for liquid samples; 0.2 mmol for solid samples). The vial was transferred into a  $\text{N}_2$  atmosphere glove box (liquid samples were subjected to three freeze-pump-thaw cycles under  $\text{N}_2$  atmosphere prior to introduction into the glove box).  $\text{Li}_2\text{O}_2$  (2.0 mmol) and  $\text{KO}_2$  (2.0 mmol) were added to the vial. For solid samples, DMF (0.5 mL) was also added. The vial was sealed, removed from the glove box, and placed in an oil bath preheated to 60 °C. The reactions were stirred for 3 days at 60 °C. After cooling to room temperature, the vial was opened, and  $d_6$ -DMSO or  $d_7$ -DMF was added (0.8 mL). The mixture was centrifuged, and the liquid layer was characterized by NMR spectroscopy.

## Results and discussion

### BANE analysis of neutral organic molecules

**1. BDEs.** The BDE of a given R-H bond provides a quantitative measurement of the stability of the radical  $\text{R}^\bullet$ ; R-H bonds with lower BDEs are more susceptible to H-abstraction. Since H-abstraction by superoxide generates  $\text{R}^\bullet$ , BDEs can be used as predictors of stability of organic molecules towards H-abstraction. The BDEs of R-H bonds in the 32 small molecules shown in Fig. 1 were computed in DMSO solvent using

B3LYP/6-31G(d,p) (Fig. 2, Table S1†), where the C-H bond in site b ( $-\text{CH}_2-$ ) of dimethoxyethane (DME) is used as a benchmark (dashed line in Fig. 2). C-H bonds adjacent to electron-withdrawing ethers are notoriously weakened by  $\sim$ 8–14 kJ mol<sup>-1</sup> compared to C-H bonds in alkanes,<sup>46</sup> and thus these compounds are susceptible to H-abstraction and subsequent decomposition (e.g., H-abstraction of ethers by  $\text{O}_2$  leads to peroxide formation<sup>47</sup>). In general, R-H bonds with higher BDEs than site b of DME should be more stable against hydrogen abstraction in the  $\text{Li}^+$ ,  $\text{O}_2$  electrode. Several points central to physical organic chemistry can be obtained from Fig. 2. First, C-H bonds of aromatic hydrocarbons have the highest BDEs (>426 kJ mol<sup>-1</sup>) among the structures studied, as the  $\text{sp}^2$ -hybridized radicals formed upon H-abstraction are very unstable.<sup>48</sup> Second, C-H bonds adjacent to atoms with  $\pi$  bonds or lone pairs of electrons that can stabilize  $\text{C}^\bullet$  through resonance, such as the allylic (25d) and benzylic (28a, 29d, 30d, and 32d) C-H bonds, amines (18b and 19d), amides (14a, 14b, 15a, 15b, 16a, 16b, 16d, 17a, 17b), and ethers, exhibit reduced BDEs compared to similarly substituted alkanes. These types of C-H bonds should be avoided wherever possible. Third, C-H BDE decreases as carbon substitution increases: primary ( $1^\circ$ ) > secondary ( $2^\circ$ ) > tertiary ( $3^\circ$ ),<sup>48</sup> with each subsequent substitution reducing the BDE by  $\sim$ 10–20 kJ mol<sup>-1</sup>. Tertiary C-H bonds (21c, 23b, 24b and 24c) should be avoided wherever possible in  $\text{Li}-\text{O}_2$  electrolyte design. Overall, from the perspective of stability against H-abstraction by superoxide, aromatic and primary or secondary alkyl C-H bonds are the most promising for electrolyte design for the  $\text{Li}^+$ ,  $\text{O}_2$  electrode.

**2. Deprotonation free energies,  $\Delta G_{\text{deprot}}$ .** The free energy of deprotonation of a given R-H bond provides a quantitative description of the acidity of that R-H bond, which is often discussed in terms of the  $pK_a$ .  $pK_a$  values for many organic molecules dissolved in water are widely available,<sup>49</sup> but values in organic solvents and the  $\text{Li}-\text{O}_2$  battery environment are less frequently tabulated. The deprotonation free energies of the R-H bonds labelled in Fig. 1, which were calculated in DMSO solvent using B3LYP/6-31G(d,p), are shown in Fig. 3. Most molecules in Fig. 1 have high  $\Delta G_{\text{deprot}}$ , i.e., they are weak acids.

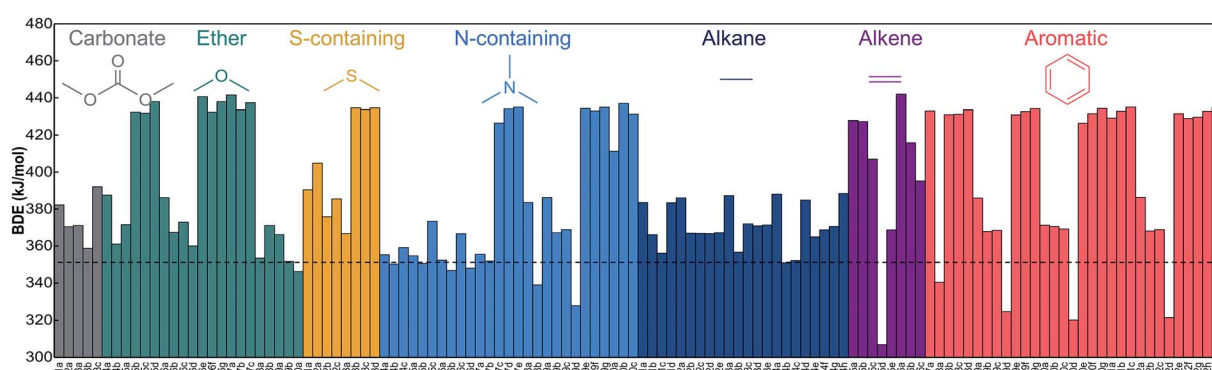
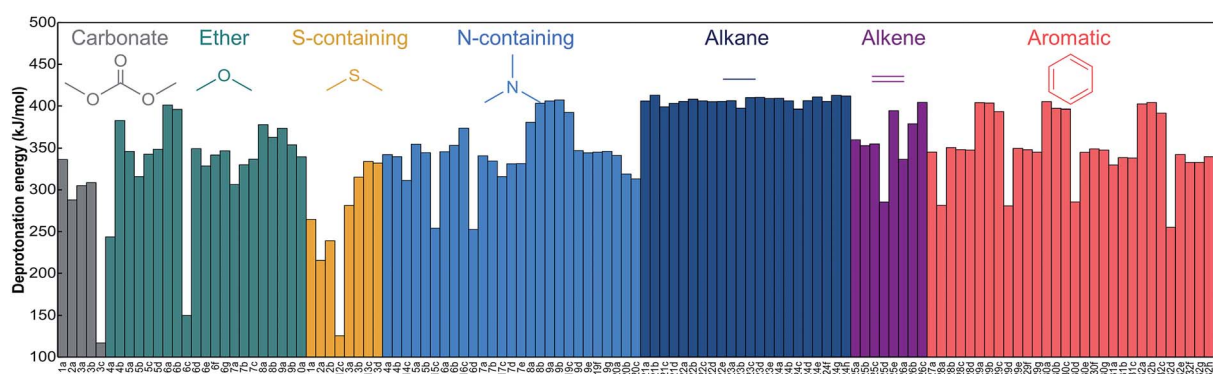


Fig. 2 BDEs of all inequivalent hydrogen atoms of the compounds shown in Fig. 1 computed at the B3LYP/6-31G(d,p) level of theory in implicit DMSO solvent. Each column represents the calculated BDE of a single carbon-hydrogen bond (see Fig. 1 for labeling). The dashed line indicates the BDE of dimethoxyethane (DME) at the  $-\text{CH}_2-$  position (9b). Hydrogens adjacent to atoms with  $\pi$  bonds or lone pairs of electrons that can stabilize  $\text{C}^\bullet$  through resonance exhibit low BDEs and are more susceptible to removal.

Of the compounds studied, alkanes have the highest  $\Delta G_{\text{deprot}}$  ( $\sim 400 \text{ kJ mol}^{-1}$ ) and hence should be the most stable against deprotonation by bases such as superoxide or peroxide in the  $\text{Li}^+$ ,  $\text{O}_2$  electrode (alkyl groups are also present in several of the ethers, N-containing, alkenes, and aromatics studied here, which gives rise to high  $\Delta G_{\text{deprot}}$  for those parts of the molecules). Our calculations show that C-H bonds adjacent to functional groups capable of resonance stabilization of the carbanion formed following deprotonation have higher acidity and lower deprotonation free energies. For example, the most acidic C-H's in DMA (**15c**) and NMP (**16d**) have the lowest  $\Delta G_{\text{deprot}}$  ( $\sim 250 \text{ kJ mol}^{-1}$ ) in N-containing compounds; this increased acidity is due to stabilization for the carbanion by the carbonyl functionality. Nevertheless, some researchers suggest that DMA and NMP are not prone to deprotonation due to their relatively high  $pK_a$ .<sup>17</sup> Additionally, EMS (**12a**) has the lowest  $\Delta G_{\text{deprot}}$  ( $\sim 215 \text{ kJ mol}^{-1}$ ) in S-containing compounds, in which case the carbanion following deprotonation is stabilized by the adjacent sulfone  $\pi$  bond(s). To prevent deprotonation, acidic C-H bonds adjacent to functional groups capable of resonance stabilization of the carbanion such as carbonyl and sulfone  $\pi$  bond(s) should be avoided in the electrolyte design.

Deprotonation involving elimination can further reduce the energy required to remove a proton from an acidic C-H. Therefore, one must also consider the possibility of elimination reactions that occur when a good leaving group is one carbon away (the “ $\beta$  position”) from the C-H bond undergoing deprotonation. For example, for PC (**3c**), nBPhE (**6c**), and EMS (**12c**), geometry optimization following deprotonation at the aforementioned site resulted in elimination (Fig. 4) as these compounds possess good leaving groups  $\beta$  to C-H bonds. Note that the energy values provided in Fig. 3 for these compounds correspond to the free energies of the elimination reaction rather than simply deprotonation, which would be limited to the free energy associated with the initial proton removal (without significant structural rearrangement of the involved molecules). Such elimination reactions were observed experimentally in polymers with this same structural motif upon exposure to  $\text{Li}_2\text{O}_2$ .<sup>21</sup>

**3. Nucleophilic substitution reaction free energies,  $\Delta G_{\text{nuc}}$ .** Electrophilic carbon atoms (*i.e.*, carbons bearing positive charge) are susceptible to nucleophilic attack by nucleophiles such as superoxide. We computed the NPA carbon atomic charges for the compounds shown in Fig. 1 and present them in Table S2;<sup>†</sup> the calculated values reflect differences in electronegativity of different atoms. For example, carbon atoms bonded to oxygen or nitrogen atoms, which are more electronegative than carbon, tend to bear partial positive charge (*e.g.*, carbonyl carbons, which are well-known electrophilic sites in organic molecules). To assess the predictive capability of carbon atomic charge on the susceptibility to nucleophilic substitution, we computed the driving force (free energy) for nucleophilic substitution by superoxide,  $\Delta G_{\text{nuc}}$ , for selected carbons (Tables 1 and S3<sup>†</sup>). A linear free energy relationship between  $\Delta G_{\text{act}}^\ddagger$  and  $\Delta G_{\text{nuc}}$  has been observed for the attack of a number of organic solvents, including carbonates, ethers, and amides,<sup>7</sup> by superoxide under the conditions present in the  $\text{Li}^+$ ,  $\text{O}_2$  electrode, which may enable faster screening of a larger chemical space *via* ground state calculations. Considering that nucleophilic substitutions are sensitive to steric effects and the presence/absence of a good leaving group, molecules with carbon atoms that are sterically less accessible to attack by superoxide, and poor leaving groups, should show greater stability towards nucleophiles. The computed  $\Delta G_{\text{nuc}}$  associated with the non-carbonyl carbons of carbonates (PC, EC, and DMC) are negative, confirming previous reports<sup>4,6,11</sup> on the vulnerability of carbonate-based electrolytes against nucleophilic substitution by superoxide. Our calculations showed that the computed  $\Delta G_{\text{nuc}}$  of these non-carbonyl carbons are of the order of  $-40 \text{ kJ mol}^{-1}$ , indicating that nucleophilic attack by superoxide at these sites has a large driving force, in agreement with previous computational studies.<sup>6,7</sup> We note that the similar values of  $\Delta G_{\text{nuc}}$  associated with these carbons (within  $12.5 \text{ kJ mol}^{-1}$ ) make it difficult to assess a hierarchy among them and can explain the differences with published computational results,<sup>6,7</sup> since the details of the calculations, such as the basis set, solvation model and initial geometry employed, could become significant within this small energy trend. It



**Fig. 3** Deprotonation free energies of all inequivalent proton sites of the compounds shown in Fig. 1 computed at the B3LYP/6-31G(d,p) level of theory in implicit DMSO solvent. Every column represents the calculated deprotonation free energy of a single proton site (with the exceptions of **3c**, **6c**, and **12c**). Base-induced elimination reaction was observed upon the removal of protons **3c**, **6c**, and **12c**; the corresponding columns represent the Gibbs free energies of the elimination reactions.

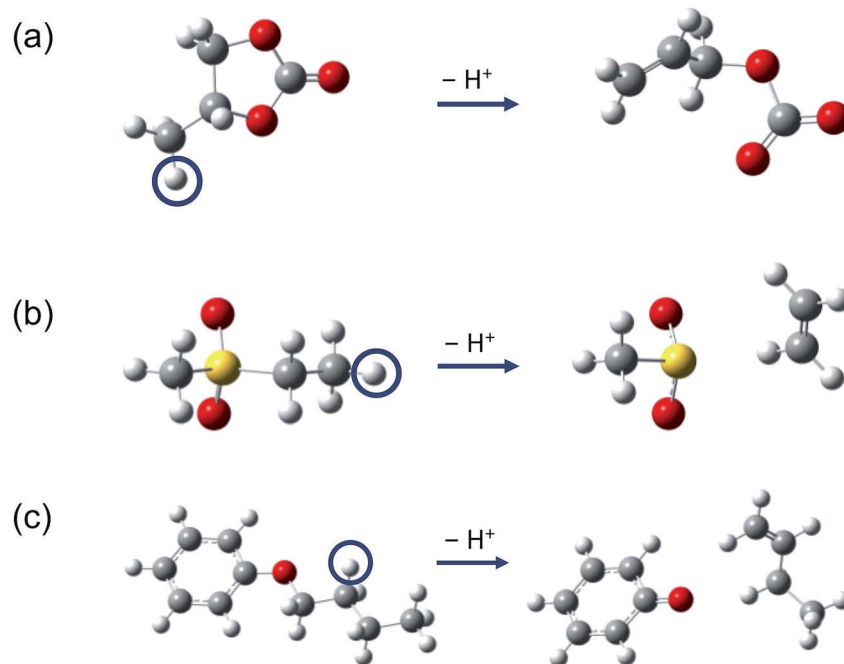


Fig. 4 Optimized structures of (a) PC, (b) EMS, and (c) nBPhE as well as their base-induced elimination reaction products. The removed protons are circled. Atom color code: red – oxygen, grey – carbon, white – hydrogen, and yellow – sulfur.

Table 1 Nucleophilic substitution free energies  $\Delta G_{nuc}$  between superoxide and selected compounds obtained at the B3LYP/6-311++G(d,p)//B3LYP/6-31G(d,p) level of theory in implicit DMSO solvent

Molecule	Carbon site	$\Delta G_{nuc}$ (kJ mol <sup>-1</sup> )
DMC	C=	93.4
DMC	CH <sub>3</sub>	-36.7
EC	C=	157.2
EC	CH <sub>2</sub>	-39.7
PC	C=	153.0
PC	CH <sub>2</sub>	-41.7
PC	CH	-49.1
MtBE	Quaternary-(O)	89.7
MtBE	CH <sub>3</sub> -(O)	82.4
MPhE	$\alpha$ -Ph-(O)	56.3
MPhE	CH <sub>3</sub> -(O)	1.8
nBPhE	$\alpha$ -Ph-(O)	100.0
nBPhE	$\alpha$ -nB-(O)	-0.61
DMF	C=	92.9
DMA	C=	88.6
NMP	C=	122.9
DMPPhA	C=	87.6
DnBPhA	$\alpha$ -Ph-(N)	50.4
DnBPhA	$\alpha$ -nB-(N)	41.4
DMSO	CH <sub>3</sub>	-2.9
EMS	CH <sub>3</sub>	-18.5
MPhS	CH <sub>3</sub>	2.9

should be noted that the trend we calculated ( $PC-CH < PC-CH_2 < EC-CH_2 < DMC-CH_3$ ) follows the overall trend in the stability of these compounds as measured experimentally (see the Procedure for Chemical Stability Test of Carbonates against KO<sub>2</sub> Section in ESI for more details†). The partial atomic charges

(Table S3†) of the carbons in Table 1 obtained by NPA in the absence of superoxide are plotted against the corresponding  $\Delta G_{nuc}$  in Fig. 5. We observe that more partially positive carbons of the studied molecules are generally less favourable attack sites for superoxide substitution (less favourable  $\Delta G_{nuc}$ ); this observation contradicts previous reports<sup>28–30</sup> on imidazolium-based ionic liquids, where the correlation between more positive carbon partial charge and higher susceptibility against nucleophilic substitution by superoxide was suggested. The researchers based their argument on the observation that the

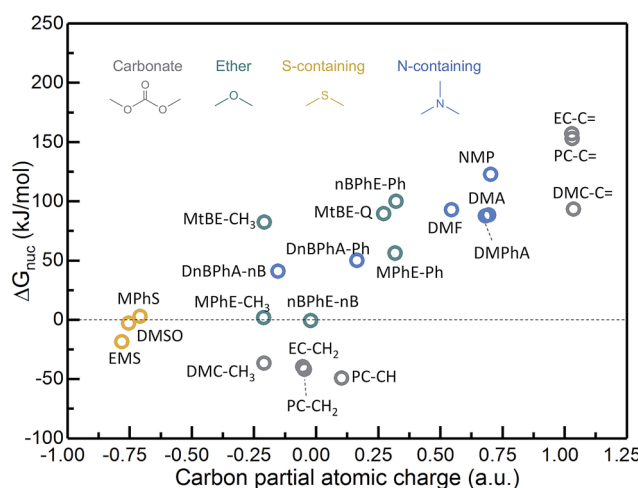


Fig. 5 Nucleophilic substitution free energies  $\Delta G_{nuc}$  at select carbon sites shown in Table 1 plotted against the partial charge of the carbon obtained by NPA in the absence of superoxide at B3LYP/6-311++G(d,p)//B3LYP/6-31G(d,p) level of theory (Table S3†).

most positive carbon (*i.e.*, the carbon that is connected to both nitrogens) of imidazolium-based ionic liquids was the preferred site for nucleophilic addition by hydroxyl anion.<sup>50</sup> However, it should be noted that such correlation might not be generalized to other nucleophilic reagents such as superoxide, as different nucleophiles could prefer to attack different carbon sites.<sup>51</sup> Therefore, we conclude that higher carbon partial positive atomic charge obtained in the absence of superoxide does not always correspond to higher nucleophilic reactivity with superoxide, in agreement with Bryantsev *et al.*<sup>7</sup> In contrast, the carbonyl carbons in the carbonates exhibit the most positive atomic charges (~1.0 a.u.), although the computed  $\Delta G_{\text{nuc}}$  indicates that nucleophilic substitution at these carbon sites is energetically unfavourable, in agreement with previous prediction (Fig. S2†).<sup>6,7</sup> These trends can be explained by comparing the stability of the leaving groups following nucleophilic substitution. The unfavourable  $\Delta G_{\text{nuc}}$  at the carbonyl carbons of carbonates can be attributed to the formation of a high energy alkoxide leaving group, whereas attack at the non-carbonyl position releases a resonance stabilized carbonate and ultimately a stable CO<sub>2</sub> molecule following decarboxylation.

The computed  $\Delta G_{\text{nuc}}$  are plotted against the increase in the partial charge of the attacking oxygen in superoxide (partial charge of the oxygen after the substitution minus its partial charge before the substitution) and the increase in the partial charge of the attacked carbon (partial charge of the attacked carbon after the substitution minus its partial charge before the substitution) in Fig. 6 and S3† (values are summarized in Table S3†). We observed that a larger increase in the partial charge of the attacking oxygen of superoxide corresponds to more favourable  $\Delta G_{\text{nuc}}$  in carbonates and ethers (Fig. 6a). The largest increases in the attacking oxygen partial charge are observed for the non-carbonyl carbons of carbonates as well as the O-alkyl  $\alpha$ -carbons of MPhE and nBPhE; these carbon sites exhibit the most favourable  $\Delta G_{\text{nuc}}$  ( $\Delta G_{\text{nuc}} < 0$ ). Furthermore, it is observed that for S- and N-containing compounds, more favourable  $\Delta G_{\text{nuc}}$  correlates with a more significant increase in the carbon partial atomic charge (Fig. 6b). We note that in these reactions, the attacked carbons' neighbours, N or S atoms, are substituted by the more electronegative O atom in superoxide, leading to the increase in carbon partial charges. These trends indicate that a larger increase in the attacking oxygen or attacked carbon partial charge is an indicator for stronger electron-donating strength of superoxide at the corresponding carbon site; this stronger electron-donating strength gives rise to more favourable  $\Delta G_{\text{nuc}}$ .

Our  $\Delta G_{\text{nuc}}$  calculations show the highest vulnerability (largest negative  $\Delta G_{\text{nuc}}$ ) against superoxide nucleophilic substitution at the  $\alpha$  carbons in nBPhE-nB, MPhE-CH<sub>3</sub>, EMS, DMSO, and MPhS; these carbon sites should be protected in the design of chemically stable electrolytes.

Importantly, several solvents with high BDEs and  $\Delta G_{\text{deprot}}$ , *e.g.*, DMSO (BDE = 390 kJ mol<sup>-1</sup> and  $\Delta G_{\text{deprot}} = 265$  kJ mol<sup>-1</sup>) and MPhS (BDE > 367 kJ mol<sup>-1</sup> and  $\Delta G_{\text{deprot}} > 281$  kJ mol<sup>-1</sup>), are susceptible to nucleophilic attack by superoxide (Table 1, Fig. 5 and Fig. S4†). These findings are in agreement with our experimental chemical stability results (Fig. 9D, S14 and S15†) and

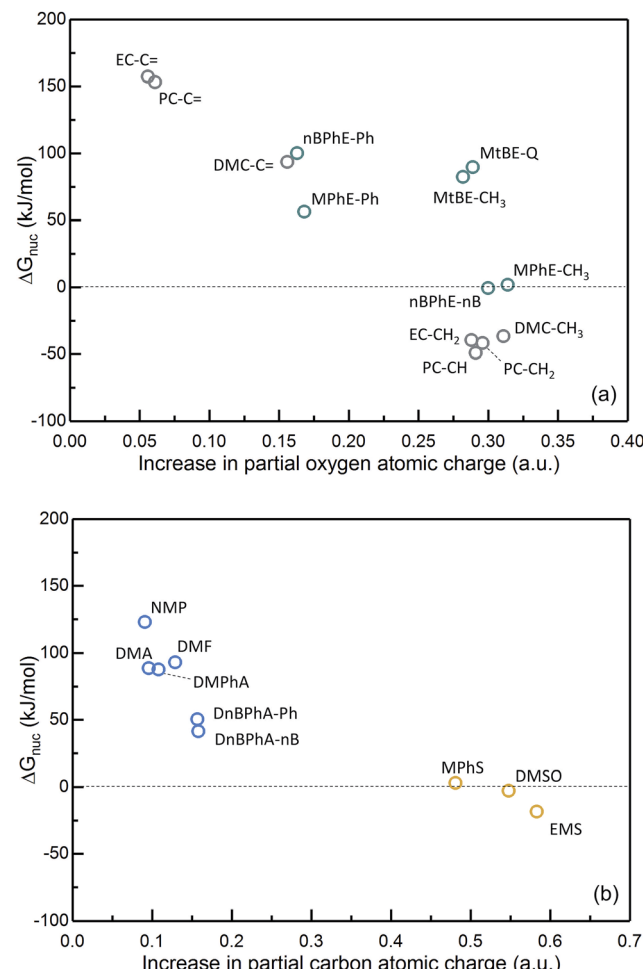


Fig. 6 Nucleophilic substitution free energies  $\Delta G_{\text{nuc}}$  at select carbon sites plotted against the (a) increase in the partial charge of the attacking oxygen in superoxide (the partial charge of the oxygen after the attack minus the partial charge before the attack) and the (b) increase in the partial charge of the attacked carbon (the partial charge of the carbon after the attack minus the partial charge before the attack) obtained at B3LYP/6-311++G(d,p)//B3LYP/6-31G(d,p) level of theory (Table S3†).

a previous report.<sup>18</sup> Therefore, it is critical to consider all three energies (BDE,  $\Delta G_{\text{deprot}}$ , and  $\Delta G_{\text{nuc}}$ ) to evaluate the chemical stability of electrolytes for Li<sup>+</sup>, O<sub>2</sub> electrodes. Overall, simple alkane and aromatic rings exhibit the highest chemical stability, whereas structures containing functional groups capable of stabilizing radicals or carbanions through resonance and unhindered  $\alpha$  carbons in O-alkyl and S-alkyl are expected to decompose in Li-O<sub>2</sub> battery environment.

**4. Oxidation potentials.** Computed adiabatic and vertical redox energies of the molecules listed in Fig. 1 using B3LYP/6-311++G(d,p)//B3LYP/6-31G(d,p) are shown in Fig. 7, Table S1† and Fig. S5.† The redox energy in eV is converted to the experimentally measured scale *versus* Li/Li<sup>+</sup> by the subtraction of 1.4 V.<sup>52,53</sup> Our computed oxidation potentials (Fig. 7) for well-known solvents, including DMC (1),<sup>32,54</sup> EC (2),<sup>32,54</sup> PC (3),<sup>31,32,54</sup> THF (8),<sup>54</sup> and DME (9),<sup>32,54</sup> are in excellent agreement with previous computational studies (Table S4†). It should be noted

that computed intrinsic oxidative potentials are typically higher than experimental values (Table S4†) due to the exclusion of interactions with salts<sup>31,32,34</sup> and electrode materials.<sup>55</sup> However, it has been demonstrated that the inclusion of the same salt anion (*e.g.*,  $\text{PF}_6^-$  or  $\text{BF}_4^-$ ) reduced the computed oxidation potentials of carbonates (*i.e.*, DMC, EC, and PC) by similar amounts.<sup>31,32,34</sup> In other words, the computed trend(s) of oxidative stability obtained in the absence of salt anions are largely similar to those obtained when the same salt anion is included. Therefore, we believe the investigation of intrinsic oxidative stability can serve as an effective screening tool.

Our calculations show that carbonates used in Li-ion batteries exhibit the highest stabilities towards electrochemical oxidation, in agreement with previous work.<sup>35,56–59</sup> In contrast, all other solvents are less stable against electrochemical oxidation than carbonates, where the computed stability voltages against electrochemical oxidation can vary from  $\sim 6.6$  to  $\sim 3.6$  V<sub>Li</sub>. Ethers have oxidation stability at voltages around  $\sim 4.5$  V<sub>Li</sub>, which are in agreement with previous experimental<sup>60–62</sup> and computational work.<sup>32,54</sup> Within S-containing solvents, sulfones have greater oxidative stability than ethers. In addition, amides (DMF, DMA, NMP, and DMPhA) have comparable stability to ethers but amines (TEA and DnBPhA) were found to be the least stable against oxidation. Moreover, alkanes and alkenes show higher stability against oxidation than ethers (Fig. S5†). It is worth noting that a special alkene structure, NBNDE (26), has lower oxidative stability due to homoconjugation, which significantly raises the alkene HOMO. Furthermore, aromatic compounds have low oxidative stability compared to ethers, and the addition of a second aromatic ring further lowers the stability towards oxidation.

The computed oxidation energies are plotted against the average of NPA partial charges of atoms that contribute to the highest occupied molecular orbitals (HOMOs) (Table S3†). The HOMOs are most dense around the carbonyl group (C=O) of

carbonates, the sulfonyl group of DMSO and EMS, and the N-C=O functionality in amides; these functional groups are also responsible for the solvation of Li<sup>+</sup>.<sup>63–65</sup> Interestingly, highly concentrated electrolytes based on PC<sup>66</sup> and DMF,<sup>65</sup> where most C=O and N-C=O are coordinated with Li<sup>+</sup> (revealed by Raman spectroscopy), exhibit improved oxidative stability, indicating that these functionalities play an important role in electrochemical oxidation. In addition, the computed HOMOs (Table S3†) are most densely located at the oxygen and aromatic carbons of aromatic ethers (for ethers without aromatic rings, the HOMOs are more evenly distributed among oxygen and carbon atoms), and the double-bonded carbons of alkenes and aromatics. Generally, increasing the average charge for atoms bearing significant HOMO density enhances the oxidative stability across different solvent families, but considerable scatter within each family is observed, as shown in Fig. 8. The significantly greater oxidation stability of carbonates than all other solvents seems to correlate with the higher positive charges of the atoms of the carbonyl group, which bear most of the HOMO density. We observed that ethers without aromatic rings are much more stable than those with aromatic rings. Finally, the oxidative stability of hydrocarbons (alkanes, alkenes, and aromatics), in spite of having almost neutral average atomic charges, can decrease significantly with increasing number of aromatic rings. It should be noted that it is important to use the charges of the atoms where the HOMOs are most densely located in this charge analysis, as simply averaging the charges of all carbons (Fig. S6†) will not yield such a correlation with oxidative stability (Fig. 8).

In summary, we note the highest oxidative stability in carbonates and alkanes and that functional groups, such as a carbonyl group, that are electron withdrawing can generally improve oxidative stability. On the contrary, structures with aromatic rings and low oxidation state sulfur atoms should be avoided or minimized in the design of stable electrolytes.

### Experimental chemical stability studies

To validate the BANE calculations in the context of the parameters listed above, we experimentally investigated the chemical stability of select compounds listed in Fig. 1 in the presence of  $\text{Li}_2\text{O}_2$  and  $\text{KO}_2$  in DMF solvent at 60 °C for 3 days. Liquid samples were directly mixed with  $\text{Li}_2\text{O}_2$  and  $\text{KO}_2$  and heated under  $\text{N}_2$  atmosphere; solid samples were dissolved in DMF before mixing with the peroxide and superoxide salts (see Experimental section for details). Since no polar solvent has been reported to be completely stable toward lithium-air battery conditions, DMF, which can dissolve all compounds of interest, was used as solvent in this study. Therefore, the stability test results presented are relative to DMF. Following heating for 3 days, the liquid phases of these reactions were analysed by NMR spectroscopy. Fig. 9 shows <sup>1</sup>H NMR spectra for 6 compounds tested (<sup>1</sup>H NMR spectra of the remaining compounds are presented in the ESI†), where compounds were deemed to be stable if there were no detectable changes in the <sup>1</sup>H NMR spectrum following mixture with  $\text{Li}_2\text{O}_2/\text{KO}_2$ . Compounds deemed unstable are underlined in Fig. 1. The <sup>1</sup>H NMR spectra of

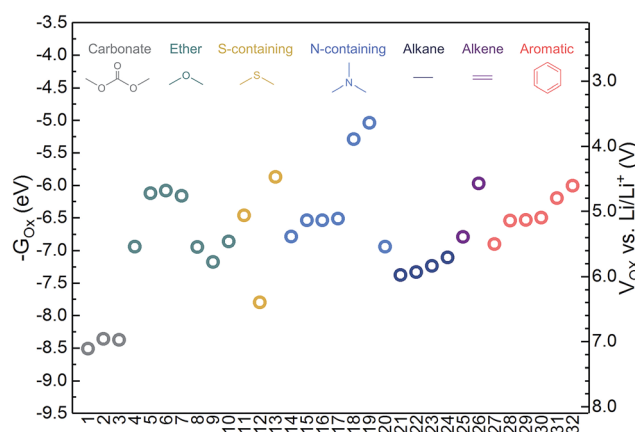
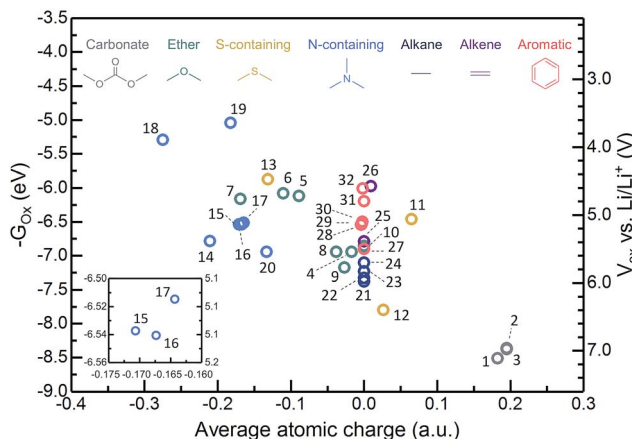


Fig. 7 Adiabatic  $-G_{\text{ox}}$  and  $V_{\text{ox}}$  of the compounds shown in Fig. 1 computed using B3LYP/6-311++G(d,p) with geometries fully optimized at B3LYP/6-31G(d,p). The oxidation energy in eV is converted to the experimentally measured scale versus Li/Li<sup>+</sup> by the subtraction of 1.4 V.<sup>52,53</sup> The converted potential vs. Li/Li<sup>+</sup> is plotted on the right axis. Carbonates show the highest oxidation potentials among the compounds considered in this study.



**Fig. 8** Adiabatic  $-G_{\text{ox}}$  and  $V_{\text{ox}}$  of the compounds shown in Fig. 1 computed using B3LYP/6-311++G(d,p) with geometries fully optimized at B3LYP/6-31G(d,p) are plotted against the average of the NPA atomic partial charges of atoms where the HOMOs are most densely located. Inset: a zoomed-in region containing compounds 15–17. The averaged NPA atomic charge is obtained by  $\bar{z} = \left( \sum_i^n z_i \right) / n$ , where  $z_i$  is the NPA partial charge of an individual atom and  $n$  is the total number of atoms considered in this charge analysis. The charges of the following atoms are considered: carbonyl carbons and oxygens ( $C=O$ ) of carbonates, all atoms that contribute to the HOMO in ethers (see Table S3† for more details), sulfur and oxygen atoms ( $S=O$ ) in DMSO and EMS, sulfur and the aromatic carbons in MPhS (the HOMO is heavily located on these carbons), nitrogens and carbonyl carbons and oxygens ( $N-C=O$ ) in amides, nitrogens and their carbon neighbours in amines and pyridine, and the double-bonded carbons of alkenes and aromatics. Additionally, the average of carbon and hydrogen charges are considered for molecules without heteroatoms.

diphenyl ether (DPhE) before (black line) and after (blue line) the stability test, are provided in (Fig. 9A), where no noticeable changes were noted. This observation is consistent with the evaluation of chemical stability using the BANE paradigm as diphenyl ether has high BDEs, high  $\Delta G_{\text{deprot}}$ , and no sites available for nucleophilic substitution in the presence of  $\text{Li}_2\text{O}_2$  and  $\text{KO}_2$ . BANE predicts that DPhE can be electrochemically oxidized at  $\sim 4.8$   $V_{\text{Li}}$ , which is consistent with experimental observation ( $\sim 4.5$   $V_{\text{Li}}$ ).<sup>37</sup>

In contrast to DPhE, carbonates DMC (1), EC (2) and PC (3) all decomposed under the testing conditions. Fig. 9B shows the <sup>1</sup>H NMR spectra for PC; differences between the before (black) and after (blue) reaction spectra are clearly observed. The observed decomposition agrees with the BANE analysis, where these compounds are susceptible to nucleophilic attack or base-induced elimination. Further agreement with the BANE analysis came from the fact that ethers with methylene groups bound to oxygen atoms, *e.g.*, nBPhE (6), THF (8), DME (9) and dioxane (10), decomposed under these reaction conditions (see Fig. 9C for exemplar spectra for DME). In contrast, ethers that only have  $\text{sp}^2$ -hybridized carbons or methyl groups attached to oxygen, *e.g.*, MtBE (4), MPhE (5) and DPhE (7), were stable. These findings confirm the previous reports that ethers such as DME and polyethylene oxide (PEO) are not suitable for electrolytes

used in  $\text{Li}^+$ ,  $\text{O}_2$  electrodes, as they are susceptible to decomposition upon hydrogen abstraction.<sup>10,21</sup> The substitution of the secondary hydrogens of DME by methyl groups is expected to increase the stability against hydrogen removal, which was observed by Nazar and coworkers.<sup>67</sup> Our experimental results suggest that methyl ether and phenyl ether groups should have enhanced chemical stability.

None of the compounds that possess sulfur-based functional groups in Fig. 1, which includes a sulfoxide (DMSO, 10, Fig. 9D), a sulfone (EMS, 11), and a thioether (MPhS, 12), were completely stable. BANE analysis predicts that DMSO<sup>18</sup> and MPhS are susceptible to nucleophilic substitution while EMS<sup>68</sup> is prone to base-induced elimination and nucleophilic substitution.

Compounds with nitrogen containing functional groups such as a formamide (DMF), an *N,N*-substituted amide (DMA, NMP, DMPhA), a tertiary amine (TEA), an aniline derivative (DnBPhA), and a heterocycle (Pyr) were examined; only DMPhA (17), TEA (18), and Pyr (20) were found stable. For example, as shown for DMA (15) in Fig. 9E, after the reaction, the peak corresponding to the proton at position *c* was dramatically changed, which could result from hydrogen-deuterium exchange due to high acidity of this C–H. Notably, this position (15c) was calculated to have a low deprotonation energy; the carbanion following deprotonation is stabilized by resonance. The observed decomposition of DMF, DMA and NMP agrees with the results of Bruce and coworkers.<sup>69</sup>

In the case of hydrocarbons, alkanes generally showed no detectable changes in the <sup>1</sup>H NMR spectra before and after exposure to these reaction conditions. In contrast, alkenes tended to undergo decomposition to complex product mixtures as exemplified by NBnde (Fig. 9F, 26). Aromatic hydrocarbons were generally stable, with the exception of cHexBen (30) which possess a weak 3° C–H bond that is susceptible to H-abstraction.

In summary, we employed the BANE framework to identify promising structures free of susceptible sites for hydrogen abstraction, deprotonation or nucleophilic substitution by superoxide radical, and our experimental analyses validated the superior chemical stability of these structures, including ethers with only  $\text{sp}^2$ -hybridized carbons or 1° carbons attached to oxygen, alkanes, and aromatics without weak 3° C–H bonds. Additionally, solvents that were deemed unstable by BANE, such as carbonates, ethers with weak C–H bonds connected to oxygen, and S-containing solvents with acidic protons or easily attacked by superoxide, have been confirmed to decompose in the experimental stability tests that mimic the chemical environment of the aprotic  $\text{Li}-\text{O}_2$  battery. Numerous molecules that exhibit chemical stability in this study such as alkanes and aromatics can have poor solvating properties, which would prevent their direct use as electrolyte solvents. However, since these structures could be incorporated into the design of new organic electrolytes (*e.g.*, polymers), we believe the assessment of their stability in this work bears significance. The learnings on what chemical moieties to be avoided in order to improve chemical stability can be used to design new electrolytes with desired chemical stability and solvating properties for aprotic  $\text{Li}-\text{O}_2$  battery.

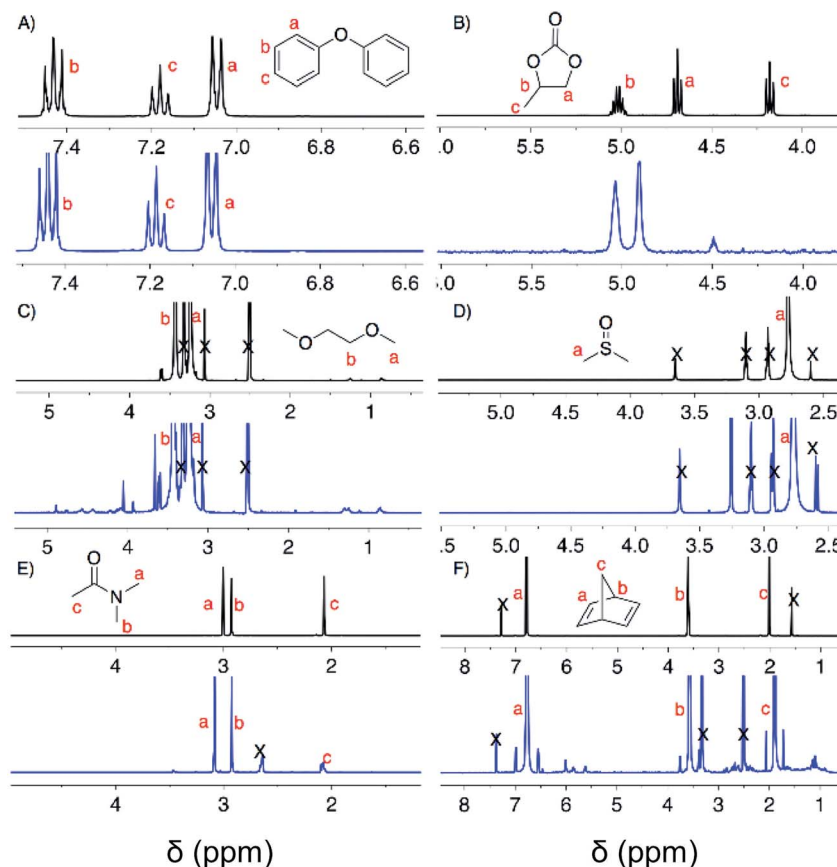


**Fig. 9** Representative  $^1\text{H}$  NMR analyses of select organic molecules. Black and blue spectra were collected before and after the chemical stability test, respectively. In the stability tests, liquid compounds were mixed with  $\text{Li}_2\text{O}_2$  and  $\text{KO}_2$  in 5 : 2 : 2 molar ratio; solid compounds were mixed with  $\text{Li}_2\text{O}_2$  and  $\text{KO}_2$  in 1 : 10 : 10 molar ratio in 0.5 mL DMF. The mixture was stirred and heated at 60 °C for 3 days. Compounds were deemed to be stable if there were no detectable changes in the  $^1\text{H}$  NMR spectrum following the reaction. Solvent peaks are indicated by 'X'.

## Conclusions

In this work, we developed a comprehensive framework, "BANE", for the global assessment of the chemical and electrochemical stability of organic electrolytes for the aprotic  $\text{Li}-\text{O}_2$  batteries. BANE is based on four stability descriptors: Bond dissociation energy (BDE), deprotonation free energy (*e.g.*, Acidity), Nucleophilic substitution free energy, and Electrochemical oxidation and reduction. We applied the BANE paradigm to several different families of organic compounds, including carbonates, ethers, N-containing molecules (amides and amines), S-containing molecules (sulfoxides, sulfones, and thioethers), alkanes, alkenes, and aromatics. Our calculations showed that the C–H bonds of aromatic hydrocarbons exhibit the highest BDEs, while alkanes are most stable against deprotonation (high  $\Delta G_{\text{deprot}}$ ). Additionally, we found that a larger increase in the partial charge of the attacking oxygen of superoxide correlates to more favourable nucleophilic substitution by superoxide in carbonates and ethers, whereas a larger increase in the partial charge of the attacked carbon correlates with more favourable nucleophilic substitution in N- and S-containing solvents. Several compounds that feature high BDEs and  $\Delta G_{\text{deprot}}$ , such as DMSO and MPhS, were found to be

vulnerable against nucleophilic substitution by superoxide, noting the importance of considering BDEs,  $\Delta G_{\text{deprot}}$  and  $\Delta G_{\text{nuc}}$  altogether when assessing the chemical stability. Furthermore, our redox calculations showed that carbonates are most stable against electrochemical oxidation and exhibit the widest electrochemical stability windows. Alkanes are also relatively stable against oxidation and reduction, whereas the addition of aromatic rings can significantly lower the electrochemical stability. The chemical stability of the 32 compounds was assessed experimentally in the presence of excess commercial  $\text{KO}_2$  and  $\text{Li}_2\text{O}_2$  at 60 °C. The experimental results are in excellent agreement with our computational predictions. The BANE approach elucidates valuable structure–property relationships that will guide the design of stable organic electrolytes for  $\text{Li}-\text{O}_2$  batteries.

## Conflicts of interest

There are no conflicts to declare.

## Acknowledgements

The authors acknowledge Samsung Advanced Institute of Technology (SAIT) for funding this research. This research used

resources of the National Energy Research Scientific Computing Center, a DOE office of Science User Facility Supported by the Office of Science of the U.S. Department of Energy under Contract No. DE-AC02-5CH11231, and the Extreme Science and Engineering Discovery Environment (XSEDE), which is supported by National Science Foundation grant number ACI-1548562. CVA was supported by the US Department of Defense through the National Defense Science and Engineering Graduate (NDSEG) Fellowship, and the Alfred P. Sloan Foundation's Minority PhD Program.

## Notes and references

- D. Aurbach, B. D. McCloskey, L. F. Nazar and P. G. Bruce, *Nat. Energy*, 2016, **1**, 16128.
- B. D. McCloskey, D. S. Bethune, R. M. Shelby, G. Girishkumar and A. C. Luntz, *J. Phys. Chem. Lett.*, 2011, **2**, 1161–1166.
- L. J. Hardwick and P. G. Bruce, *Curr. Opin. Solid State Mater. Sci.*, 2012, **16**, 178–185.
- D. Aurbach, *J. Electroanal. Chem.*, 1991, **297**, 225–244.
- F. Mizuno, S. Nakanishi, Y. Kotani, S. Yokoishi and H. Iba, *Electrochemistry*, 2010, **5**, 403–405.
- V. S. Bryantsev and M. Blanco, *J. Phys. Chem. Lett.*, 2011, **2**, 379–383.
- V. S. Bryantsev, V. Giordani, W. Walker, M. Blanco, S. Zecevic, K. Sasaki, J. Uddin, D. Addison and G. V. Chase, *J. Phys. Chem. A*, 2011, **115**, 12399–12409.
- P. G. Bruce, S. a. Freunberger, L. J. Hardwick and J.-M. Tarascon, *Nat. Mater.*, 2011, **11**, 172.
- B. D. McCloskey, R. Scheffler, A. Speidel, D. S. Bethune, R. M. Shelby and A. C. Luntz, *J. Am. Chem. Soc.*, 2011, **133**, 18038–18041.
- S. A. Freunberger, Y. Chen, N. E. Drewett, L. J. Hardwick, F. Bardé and P. G. Bruce, *Angew. Chem., Int. Ed.*, 2011, **50**, 8609–8613.
- S. A. Freunberger, Y. Chen, Z. Peng, J. M. Griffin, L. J. Hardwick, F. Bardé, P. Novák and P. G. Bruce, *J. Am. Chem. Soc.*, 2011, **133**, 8040–8047.
- W. Xu, K. Xu, V. V. Viswanathan, S. A. Towne, J. S. Hardy, J. Xiao, Z. Nie, D. Hu, D. Wang and J. Zhang, *J. Power Sources*, 2011, **196**, 9631–9639.
- W. Xu, V. V. Viswanathan, D. Wang, S. A. Towne, J. Xiao, Z. Nie, D. Hu and J. Zhang, *J. Power Sources*, 2011, **196**, 3894–3899.
- V. S. Bryantsev, J. Uddin, V. Giordani, W. Walker, D. Addison and G. V. Chase, *J. Electrochem. Soc.*, 2012, **160**, A160–A171.
- W. Xu, J. Hu, M. H. Engelhard, S. A. Towne, J. S. Hardy, J. Xiao, J. Feng, M. Y. Hu, J. Zhang, F. Ding, M. E. Gross and J. G. Zhang, *J. Power Sources*, 2012, **215**, 240–247.
- Y. Shao, S. Park, J. Xiao, J. G. Zhang, Y. Wang and J. Liu, *ACS Catal.*, 2012, **2**, 844–857.
- V. S. Bryantsev, *Chem. Phys. Lett.*, 2013, **558**, 42–47.
- D. G. Kwabi, T. P. Batcho, C. V. Amanchukwu, N. Ortiz-Vitoriano, P. Hammond, C. V. Thompson and Y. Shao-Horn, *J. Phys. Chem. Lett.*, 2014, **5**, 2850–2856.
- R. Black, S. H. Oh, J. Lee, T. Yim, B. Adams and L. F. Nazar, *J. Am. Chem. Soc.*, 2012, **134**, 2902–2905.
- E. Nasybulin, W. Xu, M. H. Engelhard, Z. Nie and X. S. Li, *J. Power Sources*, 2013, **243**, 899–907.
- C. V. Amanchukwu, J. R. Harding, Y. Shao-Horn and P. T. Hammond, *Chem. Mater.*, 2015, **27**, 550–561.
- J. R. Harding, C. V. Amanchukwu, P. T. Hammond and Y. Shao Horn, *J. Phys. Chem. C*, 2015, **119**, 6947–6955.
- K. U. Schwenke, J. Herranz, H. A. Gasteiger and M. Piana, *J. Electrochem. Soc.*, 2015, **162**, A905–A914.
- S. Das, J. Højberg, K. B. Knudsen, R. Younesi, P. Johansson, P. Norby and T. Vegge, *J. Phys. Chem. C*, 2015, **119**, 18084–18090.
- Y. Lu, H. A. Gasteiger and E. Crumlin, *J. Electrochem. Soc.*, 2010, **157**, 1016–1025.
- C. O. Laoire, S. Mukerjee, K. M. Abraham, E. J. Plichta and M. A. Hendrickson, *J. Phys. Chem. C*, 2009, **113**, 20127–20134.
- V. S. Bryantsev and F. Faglioni, *J. Phys. Chem. A*, 2012, **116**, 7128–7138.
- P. A. Hunt, B. Kirchner and T. Welton, *Chem.–Eur. J.*, 2006, **12**, 6762–6775.
- F. Mizuno, S. Nakanishi, A. Shirasawa, K. Takechi, T. Shiga, H. Nishikoori and H. Iba, *Electrochemistry*, 2011, **79**, 876–881.
- Y. Katayama, H. Onodera, M. Yamagata and T. Miura, *J. Electrochem. Soc.*, 2004, **151**, A59.
- L. Xing, O. Borodin, G. D. Smith and W. Li, *J. Phys. Chem. A*, 2011, **115**, 13896–13905.
- O. Borodin, W. Behl and T. R. Jow, *J. Phys. Chem. C*, 2013, **117**, 8661–8682.
- X. Zhang, J. K. Pugh and P. N. Ross, *J. Electrochem. Soc.*, 2001, **148**, E183.
- M. Gauthier, T. J. Carney, A. Grimaud, L. Giordano, N. Pour, H.-H. Chang, D. P. Fenning, S. F. Lux, O. Paschos, C. Bauer, F. Maglia, S. Lupart, P. Lamp and Y. Shao-Horn, *J. Phys. Chem. Lett.*, 2015, **6**, 4653–4672.
- M. Ue, M. Takeda, M. Takehara and S. Mori, *J. Electrochem. Soc.*, 1997, **144**, 2684–2688.
- K. Xu, S. P. Ding and T. R. Jow, *J. Electrochem. Sci. Technol.*, 1999, **146**, 4172–4178.
- K. Abe, Y. Ushigoe, H. Yoshitake and M. Yoshio, *J. Power Sources*, 2006, **153**, 328–335.
- T. Husch and M. Korth, *Phys. Chem. Chem. Phys.*, 2015, **17**, 22596–22603.
- M. J. Frisch, G. W. Trucks, H. B. Schlegel, G. E. Scuseria, M. A. Robb, J. R. Cheeseman, G. Scalmani, V. Barone, B. Mennucci and G. A. Petersson, *et al.*, *Gaussian 09, Revision A.02*, 2016.
- A. D. Becke, *J. Chem. Phys.*, 1993, **98**, 5648.
- C. Lee, W. Yang and R. G. Parr, *Phys. Rev. B: Condens. Matter Mater. Phys.*, 1988, **37**, 785–789.
- M. Cossi, N. Rega, G. Scalmani and V. Barone, *J. Comput. Chem.*, 2003, **24**, 669–681.
- V. Barone and M. Cossi, *J. Phys. Chem. A*, 1998, **102**, 1995–2001.
- H. J. Reich, Bordwell pK<sub>a</sub> Table (Acidity in DMSO), <https://www.chem.wisc.edu/areas/reich/pkatable/>.
- C. P. Kelly, C. J. Cramer and D. G. Truhlar, *J. Phys. Chem. B*, 2007, **111**, 408–422.

- 46 D. F. Mcmillen and D. M. Golden, *Annu. Rev. Phys. Chem.*, 1982, **33**, 493–532.
- 47 A. K. Furr, F. Wood-Black, R. Hathaway, G. W. A. Milne, H. J. Elston, R. Burke and H. J. Elston, *Chem. Health Saf.*, 2001, **8**, 38–39.
- 48 J. Clayden, N. Greeves and S. Warren, in *Organic Chemistry*, Oxford University Press, 2nd edn, 2012, p. 1026.
- 49 J. March, *Advance Organic Chemistry: Reactions, Mechanisms, and Structure*, Wiley, New York, 3rd edn, 1985.
- 50 B. M. Fernández, A. M. Reverdito, G. A. Paolucci and I. A. Perillo, *J. Heterocycl. Chem.*, 1987, **24**, 1717–1724.
- 51 J. H. Clements, *Ind. Eng. Chem. Res.*, 2003, **42**, 663–674.
- 52 L. Xing, O. Borodin, D. Smith and W. Li, *J. Phys. Chem. C*, 2011, 13896–13905.
- 53 S. T. Tti, *Pure Appl. Chem.*, 1986, **58**, 955–966.
- 54 X. Zhang, J. K. Pugh, P. N. Ross, E. Orlando and L. Berkeley, *J. Electrochem. Soc.*, 2001, **148**, E183–E188.
- 55 N. Kumar and D. J. Siegel, *J. Phys. Chem. Lett.*, 2016, **7**, 874–881.
- 56 K. Xu, *Chem. Rev.*, 2004, **104**, 4303–4417.
- 57 M. Ue, A. Murakami and S. Nakamura, *J. Electrochem. Soc.*, 2002, **149**, A1572.
- 58 D. Aurbach, Y. Gofer, M. Ben-Zion and P. Aped, *J. Electroanal. Chem.*, 1992, **339**, 451–471.
- 59 X. Zhang, R. Kostecki, T. J. Richardson, J. K. Pugh and P. N. Ross, *J. Electrochem. Soc.*, 2001, **148**, A1341.
- 60 F. Ossola, G. Pistoia, R. Seeber and P. Ugo, *Electrochim. Acta*, 1988, **33**, 47–50.
- 61 S. A. Campbell, C. Bowes and R. S. McMillan, *J. Electroanal. Chem.*, 1990, **284**, 195–204.
- 62 K. Abe, Y. Ushigoe, H. Yoshitake and M. Yoshio, *J. Power Sources*, 2006, **153**, 328–335.
- 63 K. Xu, *Chem. Rev.*, 2014, **114**, 11503–11618.
- 64 R. Tatara, D. G. Kwabi, T. P. Batcho, M. Tulodziecki, K. Watanabe, H. M. Kwon, M. L. Thomas, K. Ueno, C. V. Thompson, K. Dokko, Y. Shao-Horn and M. Watanabe, *J. Phys. Chem. C*, 2017, **121**, 9162–9172.
- 65 K. Fujii, H. Wakamatsu, Y. Todorov, N. Yoshimoto and M. Morita, *J. Phys. Chem. C*, 2016, **120**, 17196–17204.
- 66 T. Doi, R. Masuhara, M. Hashinokuchi, Y. Shimizu and M. Inaba, *Electrochim. Acta*, 2016, **209**, 219–224.
- 67 B. D. Adams, R. Black, Z. Williams, R. Fernandes, M. Cuisinier, E. J. Berg, P. Novak, G. K. Murphy and L. F. Nazar, *Adv. Energy Mater.*, 2015, **5**, 1400867.
- 68 F. Bardé, Y. Chen, L. Johnson, S. Schaltin, J. Fransaer and P. G. Bruce, *J. Phys. Chem. C*, 2014, **118**, 18892–18898.
- 69 Y. Chen, S. A. Freunberger, Z. Peng, F. Bardé and P. G. Bruce, *J. Am. Chem. Soc.*, 2012, **134**, 7952–7957.